Water Science & Technology

IWA PUBLISHING

Water Science & Technology Vol 89 No 6, 1454 doi: 10.2166/wst.2024.060

Nitrate increases the capacity of an aerobic moving-bed biofilm reactor (MBBR) for winery wastewater treatment

Patricio Walker[a], Robert Nerenberg[b], Gonzalo Pizarro[a], Marcelo Aybar[d], Juan Pablo Pavissich[e,f], Bernardo González[e,f] and Pablo Pastén[a,c,*]

[a] Departamento de Ingeniería Hidráulica y Ambiental, Facultad de Ingeniería, Pontificia Universidad Católica de Chile, Avenida Vicuña Mackenna 4860, Santiago, Chile
[b] Department of Civil and Environmental Engineering and Earth Sciences, University of Notre Dame, 156 Fitzpatrick Hall, Notre Dame, Indiana, USA
[c] Center for Sustainable Urban Development (CEDEUS), Santiago, Chile
[d] Facultad de Ingeniería y Tecnología, Universidad San Sebastián, Bellavista 7, Santiago, Chile
[e] Facultad de Ingeniería y Ciencias, Universidad Adolfo Ibáñez, Diagonal Las Torres 2640, Santiago, Chile
[f] Center of Applied Ecology and Sustainability (CAPES), Santiago, Chile
*Corresponding author. E-mail: ppasten@uc.cl

RN, 0000-0003-2203-5004; GP, 0000-0001-9554-8383; MA, 0000-0002-7716-7437; JPP, 0000-0002-7614-3572; BG, 0000-0003-1711-1471; PP, 0000-0002-9961-9342

ABSTRACT

We used bench-scale tests and mathematical modeling to explore chemical oxygen demand (COD) removal rates in a moving-bed biofilm reactor (MBBR) for winery wastewater treatment, using either urea or nitrate as a nitrogen source. With urea addition, the COD removal fluxes ranged from 34 to 45 gCOD/m^2-d. However, when nitrate was added, fluxes increased up to 65 gCOD/m^2-d, twice the amount reported for aerobic biofilms for winery wastewater treatment. A one-dimensional biofilm model, calibrated with data from respirometric tests, accurately captured the experimental results. Both experimental and modelling results suggest that nitrate significantly increased MBBR capacity by stimulating COD oxidation in the deeper, oxygen-limited regions of the biofilm. Our research suggests that the addition of nitrate, or other energetic and broadly used electron acceptors, may provide a cost-effective means of covering peak COD loads in biofilm processes for winery or another industrial wastewater treatment.

Key words: biofilms, BOD removal, denitrification, kinetics, modeling

HIGHLIGHTS

- An aerobic MBBR for winery wastewater treatment was studied.
- Kinetics and stoichiometry were determined for winery wastewater biodegradation.
- COD removal fluxes in an aerobic MBBR doubled when nitrate was added.
- Nitrate activates inner biofilm, where dissolved oxygen is limiting.
- Nitrate supplementation may provide an effective means of treating seasonal peak loads in industrial wastewaters.

GRAPHICAL ABSTRACT

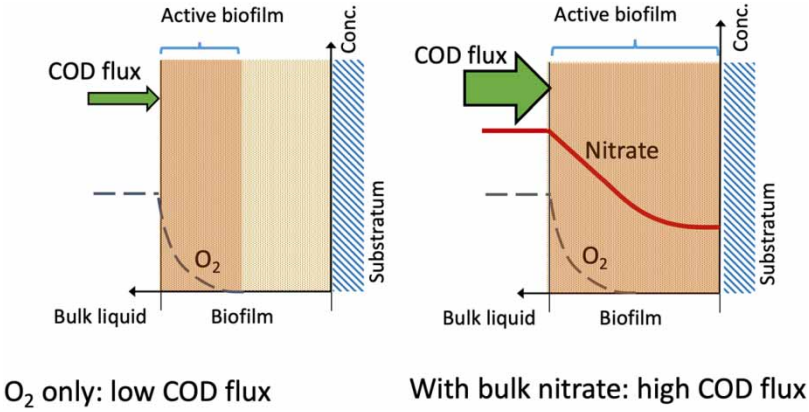

1. INTRODUCTION

A challenge with many industrial wastewaters, such as that from the winery industry, is the highly variable nature of flow rates and loadings (Chapman *et al.* 2001; Beck *et al.* 2005). Winery wastewater has high concentrations of readily biodegradable chemical oxygen demand (COD), primarily ethanol, sugars and organic acids (Chapman *et al.* 2001; Andreottola *et al.* 2005; Colin *et al.* 2005). Also, winery wastewaters are typically limited in nitrogen (N) and phosphorous (P), which are required for biological treatment (Storm 2001; Jobbágy *et al.* 2002). Ammonium or organic nitrogen is often added as the N source, due to their relatively low cost (Andreottola *et al.* 2002; Artiga *et al.* 2007).

Biofilm processes are increasingly used for winery wastewater treatment, as they can treat high COD loadings in compact reactors and can tolerate significant fluctuations in flows and loadings (Andreottola *et al.* 2005). Examples of biofilm processes for winery wastewater treatment include air-bubble column reactors, packed-bed reactors (Petruccioli *et al.* 2000), moving-bed biofilm reactors (MBBRs) (Andreottola *et al.* 2002), rotating biological contactors (Malandra *et al.* 2003), fixed-bed biofilm reactors (Andreottola *et al.* 2005), and attached growth systems based on granular sludge (Bolzonella *et al.* 2019).

Due to the low solubility of oxygen, dissolved oxygen (DO) often becomes depleted in the outer portions of the biofilm, limiting the carbon removal rates (Yu & Bishop 2001). Although aerobic processes can provide high removal rates for organics, they require costly aeration infrastructure and energy to provide the needed aeration supply rates, as well as nutrients to support biomass growth. These can result in high capital and operational costs (Bolzonella *et al.* 2019; Gupta *et al.* 2022). Supplementation with a more soluble electron acceptor, such as nitrate, can increase fluxes by allowing COD oxidation in the deeper, oxygen-limited regions of the biofilm. This was previously shown in a pilot-scale trickling filter for municipal wastewater treatment, where a nitrate spike considerably increased the substrate removal capacity (Vanhooren *et al.* 2003).

Some researchers have explored nitrate addition in suspended-growth winery treatment processes for odor control (Bories *et al.* 2007). Others have shown that winery wastewater can be used as an exogenous carbon source to drive denitrification (Rodriguez *et al.* 2007). However, no previous research has addressed nitrate addition to increase the capacity of an MBBR.

The objective of this research was to investigate the effectiveness of an aerobic MBBR for winery wastewater treatment, and the potential for enhancing COD removal by supplementing with nitrate. A bench-scale MBBR fed with synthetic winery wastewater and supplemented with urea or nitrate was operated in a continuous flow mode for over 139 days. A one-dimensional biofilm process model was developed, calibrated, and used to assess the reactor behavior.

2. METHODS

2.1. Synthetic winery wastewater

Synthetic winery wastewater was used, following Chapman *et al.* (2001). The influent contained glucose (694 mgCOD/L), sucrose (853 mgCOD/L), tartaric acid (122 mgCOD/L), lactic acid (91 mgCOD/L), acetic acid (43 mgCOD/L), and diluted wine (0.01 ppv, 2,548 mgCOD/L). The theoretical COD was 4,351 mg/L. Nitrogen concentrations and organic loadings are shown in Table 1.

Table 1 | Hydraulic retention time (HRT), organic loading, and nitrogen dosage used to test the laboratory-scale reactor

Day	HRT (h)	Organic loading (gCOD/m^3-d)	Nitrogen dose (gCOD/gN)	Nitrogen form
1–70	25	3.5	100/1.1	Ammonium
71–96			100/3.2	Nitrate
97–107	9	9.7	100/3.2	
108–115			100/7.9	
116–125			100/7.9	Urea
126–139			100/7.9	Nitrate

2.2. Laboratory-scale reactor setup

A glass bioreactor with a working volume of 10 L was filled to 60% of its volume with plastic media carriers (Figure 1). The carrier specific surface area was 240 m^2/m^3, considering only the internal area of the carriers, and the density was 0.93 g/cm^3. The effective bulk liquid working volume was 8.6 L and the available specific area in the carriers was 144 m^2/m^3. Settled sludge (600 mL) from a winery wastewater treatment plant in the Central Valley of Chile was used as the inoculum.

The experimental setup is shown in Figure 2. The influent was titrated with 0.5 N sodium hydroxide in a 50 mL mixing chamber to maintain an influent pH between 6 and 7. The mixing proportions and flows were adjusted using Masterflex L/S peristaltic pumps (Cole-Parmer, Chicago, IL, USA). Two membrane air diffusers provided continuous aeration. The airflow rate provided complete mixing of carriers and aeration. The experiments were carried out at room temperature (20 $\pm$ 3 °C).

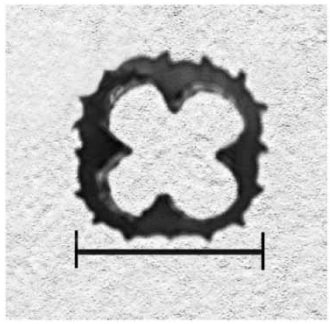

Figure 1 | Biomass carrier (scale bar: 1 cm; specific surface: 240 m^2/m^3; density: 0.93 g/cm^3).

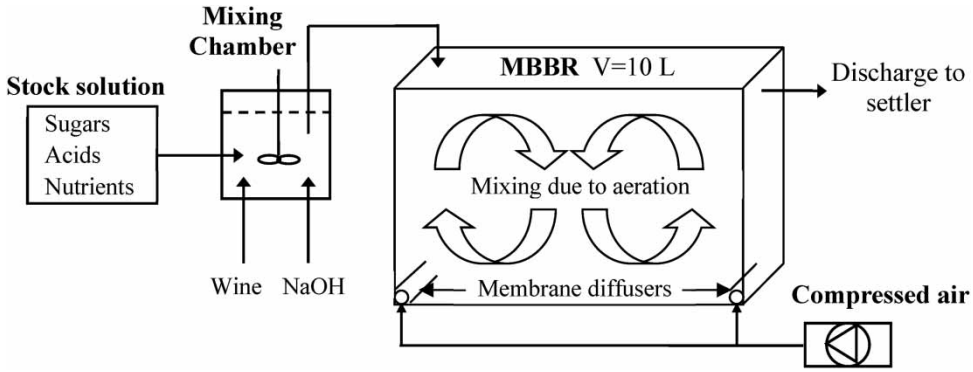

Figure 2 | Setup of the laboratory scale MBBR. A stock nutrient solution was mixed with diluted wine to mimic a typical winery wastewater. Sodium hydroxide was used to keep the effluent pH between 6 and 7. Two membrane diffusers provided aeration and mixing.

2.3. Laboratory-scale reactor testing

The reactor initially was run with a hydraulic retention time (HRT) of 25 h. Subsequently, the HRT was decreased to 9 h (Table 1). The nitrogen source was varied as shown in Table 1. The typical phosphorous requirement for heterotrophic growth is 1 mgP/gCOD. The phosphorous dosage was 0.6 mgP/gCOD through day 70, resulting in phosphorus limitation. After day 70, it was increased to above 3 mgP/gCOD.

2.4. Mathematical model

A mathematical model was developed based on the Activated Sludge Model No. 1 (ASM1) (Henze *et al.* 1987). The model's processes and stoichiometry are summarized in Table 2. Model components are readily biodegradable substrate (S_{S1}), slowly biodegradable substrate (X_S), active heterotrophic biomass (X_H), products from biomass decay (X_P), DO (S_O) and nitrogen (ammonium or nitrate; S_N). The model included a single microbial species, heterotrophic bacteria, carrying out aerobic or anoxic respiration, growth, and decay. Hydrolysis of entrapped particulate organic compounds was also included. Since ASM1 does not include nutrient limitation nor the use of nitrate as nitrogen source, the following modifications were made: (i) the same state variable, S_N, was used to represent ammonium or nitrate, as they were never used concurrently; (ii) microorganisms could use either nitrate or ammonium as the nitrogen source with the same stoichiometry; (iii) an extra Monod term was added for nitrogen, to prevent growth when nitrogen was limiting.

The model described in Table 2 was implemented in the computer program AQUASIM 2.1 (Reichert 1998). AQUASIM includes a one-dimensional biofilm model (Wanner & Morgenroth 2004). It allows for multiple substrates and microbial species to be modeled, and also provides a parameter estimation routine (Wanner & Gujer 1986; Wanner & Reichert 1996; Reichert & Wanner 1997). The parameters for the model were determined from measured data, parameter estimation from respirometry tests, reactor performance, and the literature (Table 3). It was assumed that the same kinetic parameters applied to bacteria in suspension and in the biofilm. The biofilm model was set for a confined reactor, a rigid biofilm matrix, and with biofilm pores filled by liquid only. The biofilm area was the internal area of carriers in the experimental MBBR. A global surface detachment rate was assumed, proportional to biofilm growth, until the observed biofilm thickness of 1.2 mm was achieved. At that point, the detachment velocity was set to the growth velocity, keeping the biofilm thickness constant.

2.5. Respirometry tests

Respirometry tests were conducted, following the static gas, static liquid principle (Spanjers *et al.* 1998), in a 300 mL respirometer. Temperature was kept at 20 ± 1 °C with a water bath, and a magnetic stirrer provided complete mixing. Aeration was provided by an air pump connected to aeration stones. During tests, the system was first saturated with oxygen, and then DO depletion was monitored to 1.5–2 mg/L. This process was repeated until an endogenous baseline was reached. DO was measured in the bulk liquid with an online fluorescence oxygen probe (LDO101, Hach Lange, Loveland, CO, USA), connected to a digital meter (HQ40d, Hach Lange, Loveland, CO, USA).

Three types of experiments were conducted, depending on the characteristics of the biomass. The objective was to independently test the response of suspended biomass only (Experiment 1), attached biomass only (Experiment 2), and attached biomass plus suspended biomass (Experiment 3). In all cases, biomass was aerated for at least 16 h before starting the

Table 2 | Model process matrix

	S_{S1}	X_S	X_H	X_P	S_O	S_N	Process rate
Process							
Aerobic growth of heterotrophs on S_{S1}	$-\frac{1}{Y_1}$		1		$-\frac{1-Y_1}{Y_1}$	$-i_{XB}$	$\hat{u}_H \frac{S_{S1}}{K_{S1}+S_{S1}} \frac{S_O}{K_{OH}+S_O} \frac{S_N}{S_N+0.001} X_H$
Anoxic growth of heterotrophs on S_{S1}	$-\frac{1}{Y_1}$		1			$-\frac{1-Y_1}{2.86Y_1}-i_{XB}$	$\hat{u}_H \frac{S_{S1}}{K_{S1}+S_{S1}} \frac{K_{OH}}{K_{OH}+S_O} \frac{S_N}{K_{NO}+S_N} n_g \cdot X_H \cdot \phi$
Decay of heterotrophs		$1-f_P$	-1	f_P			bX_H
Hydrolysis of entrapped organics	1	-1					$k_H \frac{X_S/X_H}{k_X+X_S/X_H} \left[\frac{S_O}{K_{OH}+S_O}+n_h \frac{K_{OH}}{K_{OH}+S_O} \frac{S_{NO}}{K_{NO}+S_{NO}}\right] X_H$

If ammonium or urea is added, $\phi = 0$; if nitrate is added, $\phi = 1$.

Table 3 | Parameters used for the simulation of the MBBR

Symbol	Parameter	Value	Unit	Source
Stoichiometry				
Y_1	Yield for readily biodegradable substrate S_{S1}	0.67	gcell COD/gCOD oxidized	Respirometry experiments
f_P	Fraction of biomass yielding decay	0.08	_	Henze *et al.* (1987)
i_{XB}	Mass of nitrogen in biomass	0.043	gN/gCOD in biomass	Calibration with reactor data
Kinetics				
$\hat{u}_h$	Specific growth rate	1.77	1/day	Respirometry experiments
K_{S1}	S_{S1} half-rate constant	4.38	gCOD/m^3	Respirometry experiments
K_{OH}	Oxygen half-rate constant	0.20	gO_2/m^3	Henze *et al.* (1987)
K_N	Nitrogen (nitrate) half-rate constant	0.50	gN/m^3	Henze *et al.* (1987)
b	Decay rate	0.16	1/day	Calibration with reactor data
n_g	Correction factor for anoxic growth	0.80	_	Henze *et al.* (1987)
K_H	Hydrolysis of entrapped organics	3.00	gslow COD/gcellCOD-day	Henze *et al.* (1987)
K_X	Hydrolysis of entrapped organics	0.03	gslow COD/gcellCOD-day	Henze *et al.* (1987)
n_h	Correction factor for anoxic hydrolysis	0.40	_	Henze *et al.* (1987)
Biofilm				
D_S	Soluble substrate diffusion in water (ethanol)	1.1×10^{-4}	m^2/day	Perry & Green (1997)
D_O	Oxygen diffusion in pore water	1.7×10^{-4}	m^2/day	Perry & Green (1997)
D_N	Nitrogen (nitrate) diffusion in pore water	2.6×10^{-4}	m^2/day	Perry & Green (1997)
ρ	Bacterial density	128	kg/m^3	Calibration with reactor data

respirometry tests, to achieve the endogenous phase. Biomass samples were taken from the bioreactor at the end of the reactor operation (day 139).

Experiment 1: A 290-mL sample of mixed liquor suspended solids (MLSS) was taken from the MBBR (818 mgVSS/L) and then tested with successive spikes of 15, 30, 45, and 60 mgCOD/L of synthetic wastewater.

Experiment 2: A sample of 100 carriers was withdrawn from the MBBR (5.2 g of solids) and washed carefully with deionized water to avoid detachment. The carriers with attached biofilm were then transferred to a respirometer with enough filtered mixed liquor to fill a total of 290 mL. Tests were conducted with successive spikes of 15, 30, and 45 mgCOD/L of synthetic wastewater.

Experiment 3: The same 100 carriers of Experiment 2 were transferred to a volume of unfiltered MLSS (1,100 mgVSS/L) to fill 290 mL in the respirometer. Tests were conducted with successive spikes of 15, 30, 45, 60 and 75 mgCOD/L of synthetic wastewater.

2.6. Analytical methods

Total suspended solids (TSS) were calculated following the standard methods procedure for total solids (APHA 2005). Total attached solids (TAS) were estimated with a sample of ten carriers taken from the MBBR. The sample carriers were dried at 105 °C, and then weighed. The attached solids were washed by mechanical brushing and carriers were cleansed with tap water and kept in an acid solution (10% HCl) for at least 12 h. Clean carriers were washed with deionized water, dried at 105 °C and then weighed. Finally, TAS were calculated following Equation (1):

$$\text{TAS} = (A - B) \cdot \frac{\text{TC}}{B} \cdot 100 \text{ [mg/L]} \quad (1)$$

where TC is the total mass of carriers in the reactor (1,486 g), A is the mass of sample carriers plus dried attached biomass (g), and B is the mass of clean sample carriers (g).

COD (influent and effluent), TSS, and TAS were analyzed every 2–3 days. The analyses were performed on the soluble COD fraction (sCOD), filtered with a 0.45-μm Millipore filter, using a commercial colorimetric method (Hach COD

0–1500 ppm digestion vials and Hach DR/2010 Spectrophotometer, Loveland, CO, USA). Solids were estimated as described above. Wastewater flow rates and pH (9157BN electrode, Thermo Orion, Beverly, MA, USA) were measured twice a day.

3. RESULTS AND DISCUSSION

3.1. Respirometry tests and parameter estimation

The responses of suspended biomass only (Experiment 1), attached biomass only (Experiment 2), and attached biomass mixed plus suspended biomass (Experiment 3) to spikes of synthetic wastewater are shown in Figure 3. Simulations were performed using the mathematical model described in Section 2.4 accounting for two modelling scenarios: (i) oxygen is set as a non-rate-limiting substrate, even within the biofilm (Figure 3(a)–3(c)) and (ii) the bulk oxygen concentrations used in the model are those measured in real time during each experiment, so oxygen may be rate-limiting depending on each experimental condition (Figure 3(a)–3(c)).

Stoichiometry (yield for readily biodegradable substrate Y_1) was obtained from each respirogram and resulted in 0.63, 0.72 and 0.67 [gcellCOD/gCOD oxidized] for Experiments 1, 2, and 3, respectively. The value obtained from Experiment 3 was

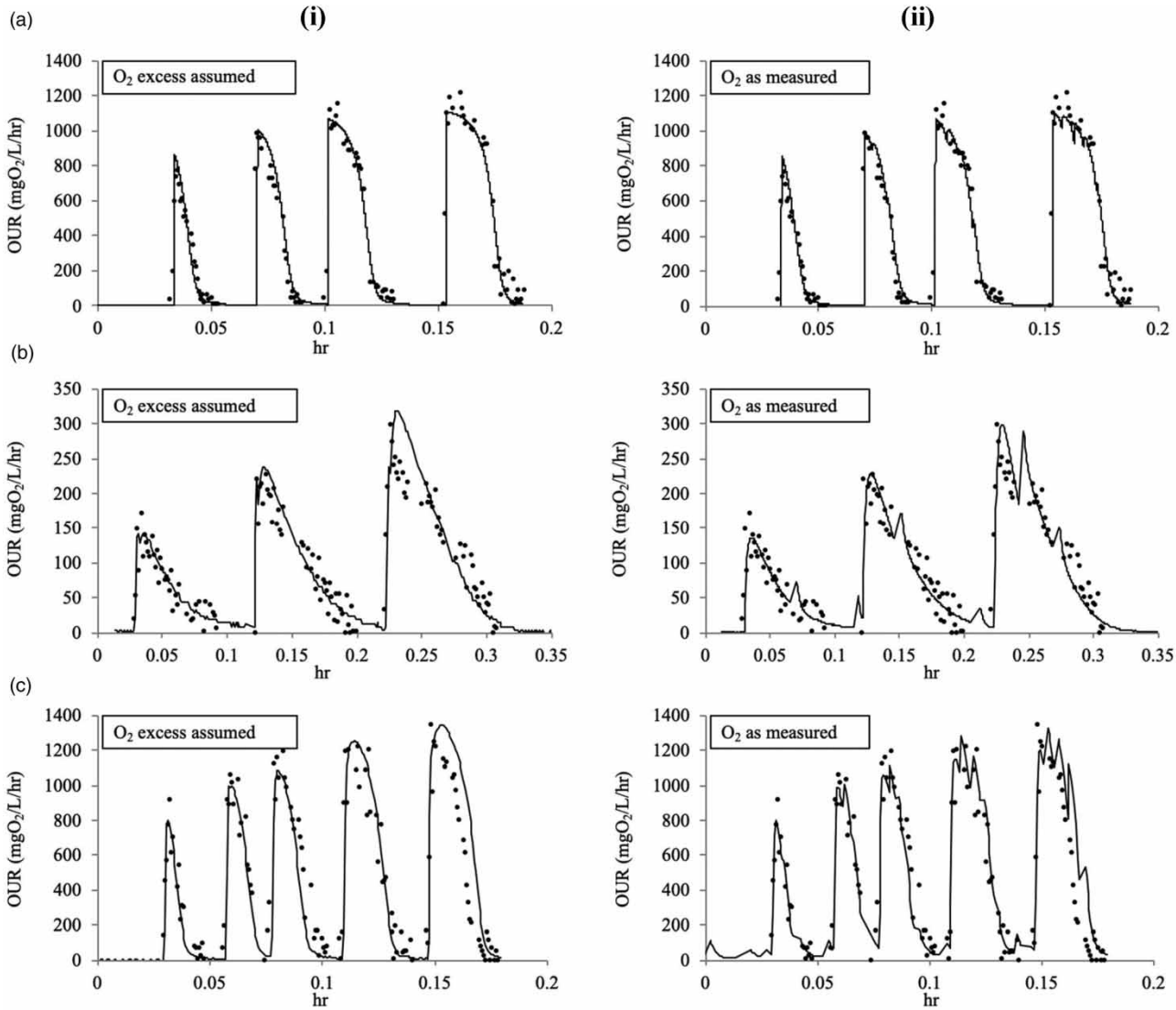

Figure 3 | Measured (dots) and simulated (lines) oxygen uptake ratio (OUR) of (a) Experiment 1 mixed liquor suspended solids (MLSS), (b) Experiment 2 (carriers), (c) Experiment 3 (MLSS + carriers). In the figures on the left, the modeled rates neglect oxygen limitation (i), while on the right the model assumes oxygen limitation as measured (ii).

further used to model the MBBR because it represented the closest condition to actual MBBR environment, which includes both suspended and attached biomass.

Kinetic parameters (specific growth $\hat{u}_h$ and half-rate constant K_{S1}) were estimated using the AQUASIM parameter estimation routine in Experiment 1. Results are shown in Table 3. Experiments 2 and 3 were used to validate kinetic parameters obtained from Experiment 1 and to assess the effect of oxygen limitation within the biofilm.

The fractionation of synthetic wastewater COD was also evaluated. The mean influent sCOD was 4,338 mg/L (see Table 4), which is 99.7% of the total theoretical COD. Given that the influent COD was almost 100% soluble, the inert particulate fraction (X_I) and active biomass (X_H) were assumed negligible and a value of 0 was used. The readily biodegradable substrate, S_{S1}, was estimated from respirometry tests as 85% of the total sCOD. The inert soluble fraction (S_I) was estimated as 3% of the influent sCOD, given that the maximum sCOD removal observed for the MBBR was 97%. Finally, the slowly biodegradable substrate fraction (X_S) was 12%, by difference. This fractionation was similar to that obtained in previous research on winery wastewater (Beck *et al.* 2005).

The model provided a good fit to all three experiments (Figure 3), supporting the assumption that one set of kinetic parameters can be used to model suspended and attached biomass. As expected, the results from Experiment 1 suggested that oxygen limitation was not important when only suspended biomass was present, since oxygen was always above 1.5 mg/L. This can be seen in Figure 3(a), where the fit is the same with or without modelling oxygen limitation. However, Experiments 2 and 3 suggest that oxygen is limiting within the biofilm. This can be observed in Figure 3(b) and 3(c), where the fit is slightly better when oxygen limitation is included in the model.

3.2. Lab scale MBBR performance

A summary of the performance of the reactor and the organic loads applied during the experimental evaluation are shown in Table 4.

The COD input and outputs are shown in Figure 4. Over 90% COD removal was achieved by day 13, with COD removal fluxes around 22 gCOD/m^2-d. At the end of the third week, severe viscous bulking began, and efficiency started to decrease. Efficiencies less than 70% were attained and fluxes decreased to 15–20 gCOD/m^2-d. Viscous bulking is commonly associated with nutrient deficiency (Jenkins *et al.* 2003) and has been documented for winery wastewater (Jobbágy *et al.* 2002). The viscous bulking development can be explained by the low initial nutrient dosage, especially for nitrogen (mass ratio COD/N/P = 100/1.1/0.6).

Following supplementary nutrient addition at day 70 (COD/N/P = 100/3.15/3.25), the viscous bulking ceased and the removal efficiency increased to an average of 95%, or approximately 23 gCOD/m^2-d, between days 85 and 97 (Figure 4). At this point, achievement of the steady state was assumed and the HRT was reduced from 25 to 9 h. Another episode of viscous bulking occurred, probably due to the shock loading caused by decreased HRT. This diminished the removal efficiencies to 70%, although the removal fluxes increased to 46 gCOD/m^2-d due to the higher loading. The nutrient concentration was increased on day 108 (COD/N/P = 100/7.9/4.9). The bulking ceased and the removal fluxes increased to around 60 gCOD/m^2-d. From day 115 to 125, nitrate was replaced with an equivalent amount of urea (Table 1 and Figure 4). While no bulking was observed, the removals decreased to 50–63%, or 34–45 gCOD/m^2-d. When returning to nitrate, between days 128 and 136, the removal efficiencies increased again to an average of 96% with no bulking episodes, and the removal

Table 4 | Experimental MBBR performance for COD removal

		HRT = 25 h	HRT = 9 h
Influent COD	mg/L	4,338 ± 298	
Effluent COD	mg/L	762 ± 848	886 ± 674
Applied COD load	kgCOD/m^3-d	3.5	9.7
	gCOD/m^2-d	24.6	67.5
Removal COD flux	gCOD/m^2-d (mean)	20.4	54.3
	gCOD/m^2-d (min.)	15.4[1]	34.2
	gCOD/m^2-d (max.)	23.9	65.8

[1]Excluding the first week of operation.

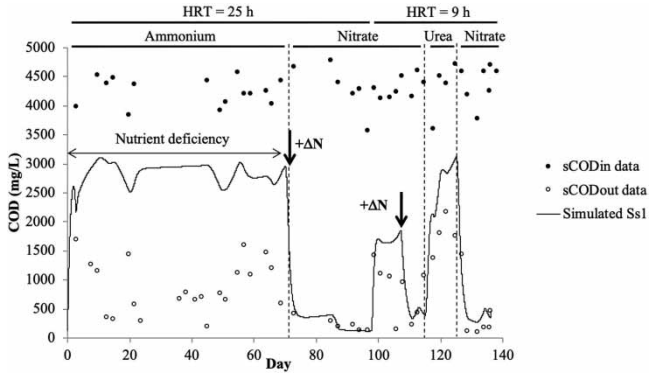

Figure 4 | Influent, effluent and simulated COD. Changes in hydraulic retention time (HRT) and in nitrogen source and dose (+ΔN) are also shown.

fluxes increased near to 65 gCOD/m^2-d. At this point, achievement of the steady state was assumed again and the experiment concluded.

Maximum removal rates for MBBRs are typically 25–35 gCOD/m^2-d, and the recommended design flux is 30 gCOD/m^2-d (Ødegaard *et al.* 2000). Aygun *et al.* (2008) tested loadings up to 96 gCOD/m^2-d and obtained a maximum removal rate of 43 gCOD/m^2-d (45% efficiency). In the case of winery wastewater, loads around 30 gCOD/m^2-d have been tested in biofilm treatment systems yielding maximum removal efficiencies near 100% (Andreottola *et al.* 2009). In our experiments, the highest loading was 67 gCOD/m^2-d. When urea was added as N source, the removal rate was 34–45 gCOD/m^2-d, similar to the previously reported values. However, when nitrate was added, fluxes increased up to 65 gCOD/m^2-d. As explained by Vanhooren *et al.* (2003), denitrification can be induced by adding nitrate, increasing considerably substrate removal capacity. As discussed in the following sections, the enhancement of COD removals with nitrate addition is further supported by our modelling.

3.3. Lab scale MBBR modelling

A dynamic simulation was carried out using the model described in Section 2.4. Results showed that simulations overestimated the effluent COD when there was nutrient limitation (Figure 4). The model assumes that no growth or COD removal occurs when nutrients are deficient. However, it has been proposed that microorganisms react to a nutrient deficiency by shifting their metabolism to produce extracellular polysaccharides (EPS), which has low concentrations of nitrogen and phosphorus, instead of other cell materials (Jenkins *et al.* 2003). This means that under nutrient limitation, substrate oxidation is not completely inhibited and there is a certain degree of solids production (EPS), which can be also the cause of viscous bulking. This difference between the model and the actual behavior presumably leads simulations to overestimate COD (Figure 4) and underestimate solids due to EPS formation (see Supplementary Material, Figures S1 and S2).

Following the initial nutrient deficiency period (days 0–70), the model correctly reproduced the COD profile in the reactor, even accounting for the effects resulting from the change in HRT (from 25 to 9 h) and the use of urea instead of nitrate (Figure 4). In particular, when HRT was set to 9 h and nutrient dosage was COD/N = 100/7.9 (from days 108 to 139), the model was able to reproduce the decrease in COD removal due to switching from nitrate to urea as N source. This is explained by denitrification in the deeper portions of the biofilm, leading to an increase in COD oxidation activity, as is shown in Section 3.4.

During the viscous bulking episode, simulations underestimated TSS as resulted in calculated values 35% lower than measured, in average. When no bulking occurred, the model reproduced the TSS trends, even accounting for the change in HRT (from 25 to 9 h), and the use of urea instead of nitrate. TAS were typically underestimated by the model, but for HRT = 25 h they were in the correct order of magnitude. However, for HRT = 9 h, TAS reached values 15–20 times higher than predicted, and finally values over 30,000 mg/L, were produced. This suggests that the biofilm density increased when denitrification took place, since no substantial changes were observed in biofilm thickness. It is possible that changes in the biofilm internal structure occurred due to the high denitrification activity (see Section 3.4), which allowed the anoxic

growth of bacteria in deeper zones of the biofilm, thus generating a denser biofilm. Another possibility is that the biofilm accumulated a significant amount of inert material.

3.4. Model predictions

The biofilm model was used to gain insights into the effects of nitrate addition. The simulated oxygen and nitrate profiles in the biofilm are shown in Figure 5(a), for the case when nitrate is supplied in the bulk. The oxygen profiles without nitrate are essentially the same (data not shown). COD uptake rates in the biofilm, with and without nitrate, are shown in Figure 5(b). The results suggest that nitrate addition greatly enhances substrate uptake in the deeper portions of biofilm, significantly increasing the overall COD flux into the biofilm. Those are essentially the same results obtained by Vanhooren *et al.* (2003), who modeled a highly loaded trickling filter after adding a pulse of nitrate. In our simulations, for example, the COD removal flux with urea (day 122) was 24 gCOD/m^2-d. But by simply adding nitrate, the simulated flux more than doubled to 54 gCOD/m^2-d (day 131).

3.5. Sensitivity analysis

A sensitivity analysis was carried out with the reactor model using soluble COD input and output data. The most sensitive parameters were specific growth rate ($\hat{u}_h$) and the mass of nitrogen in biomass (i_{xb}). Decay rate (b) and bacterial density (rho) had a small effect, meanwhile the yield for readily biodegradable substrate (Y_1) and the half-rate constant for readily substrate (K_{S1}) had almost no effect (see Supplementary Material, Figures S3–S5). In every scenario tested, the model showed a contribution of denitrification to COD removal, the difference was only its magnitude compared to aerobic oxidation. A better fit can be obtained if $\hat{u}_h$ is assumed to be 20% higher than that was found in respirometry tests (R^2 from 0.73 to 0.74). In respirometry tests COD was present in lower concentrations than in the MBBR, thus it is possible that $\hat{u}_h$ was underestimated.

3.6. Assessment of nitrate addition strategy

The calibrated model was used to predict the reactor's performance when ammonium (urea) or nitrate is added at different doses. A hypothetical operation scenario was set with an HRT of 9 h and influent COD spikes of 1,000, 2,000, 3,000, 4,000, 5,000, 6,000, 7,000 and 8,000 mgCOD/L (Table 5).

Results for COD are shown in Figure 6. The bulk DO was simulated close to saturation (between 7 and 8 mg/L).

At a loading rate of 20 gCOD/m^2-d, there are no differences between urea and nitrate because the process is COD limited, not oxygen limited. At higher COD loadings, oxygen limitation occurs and differences in COD removal rate can be observed depending on the nitrogen source and quantity added. If ammonium is added in excess, the COD removal rate reaches a maximum of around 25 gCOD/m^2-d. With nitrate, the model predicts a maximum removal rate of 63 gCOD/m^2-d. If the process efficiency is set at 90%, the maximum design loading rate would be near 60 gCOD/m^2-d according to the model. This is

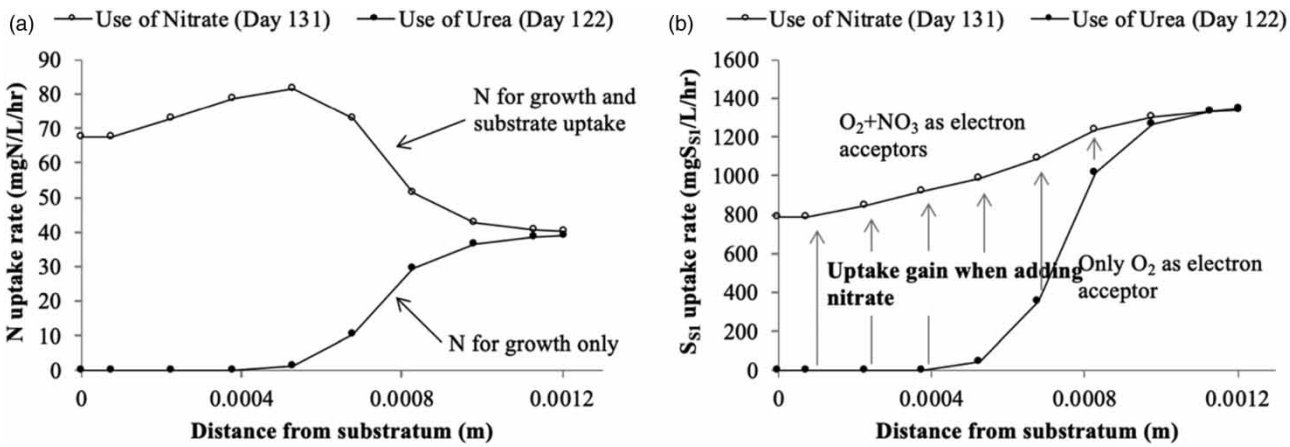

Figure 5 | (a) Model-predicted N uptake rates profiles in biofilm and (b) substrate uptake rate profiles in biofilm. The presence of nitrate allows COD uptake deep in the biofilm, providing higher overall activity and higher S_{S1} fluxes.

Table 5 | Hypothetical operation scenarios tested and results for COD

	COD input (mg/L)				
	1,000	2,000	3,000	4,000	5,000
Nitrogen type – dose	**COD output (mg/L)**				
Ammonium – COD/N = 100/8	14.4	23.5	24.3	24.7	25.1
Nitrate – COD/N = 100/4	14.4	28.0	34.9	41.2	47.5
Nitrate – COD/N = 100/6	14.4	28.7	42.6	53.6	61.8
Nitrate – COD/N = 100/8	14.4	28.7	42.7	56.3	62.9

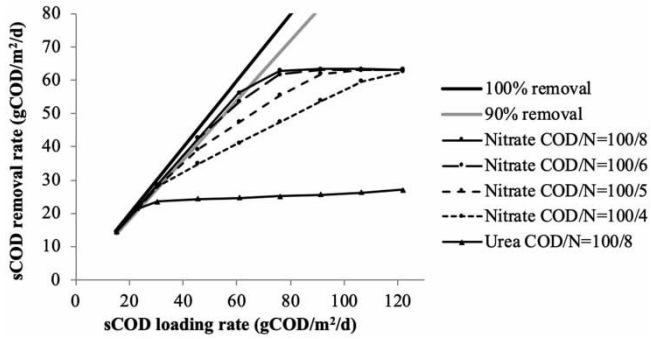

Figure 6 | MBBR performance in hypothetical operation scenarios. Ammonium is tested as nutrient source when added in excess (dose: COD/N = 100/8) compared to nitrate when added in excess (dose: COD/N = 100/8) and in lower doses (COD/N = 100/6, COD/N = 100/5 and COD/N = 100/4).

approximately double what has been observed for aerobic biofilm systems for winery wastewater treatment (Andreottola *et al.* 2009).

The above assessment suggests that high-rate aerobic biofilm systems can experience major capacity improvements if nitrate is properly dosed. As pointed out by Vanhooren *et al.* (2003), the continuous use of nitrate may not be economically feasible. However, a more cost-effective solution may be to add nitrate during peak loads only. If peak loads can be 'shaved' by nitrate addition, the reactor size can be minimized. While valid for any type of process, this is particularly interesting for winery wastewater treatment, where there are substantial peak loading events during the wine season (Bolzonella *et al.* 2019).

When choosing the nitrate dose, there is a tradeoff between improving COD removal and creating excess effluent nitrate. Modelling suggests that a COD/N = 100/6 dose may be the best choice. For future research, it is important to assess the effects of biofilm thickness on the effectiveness of this approach. For example, if a thin biofilm allows full penetration of oxygen, the nitrate addition strategy will not be effective. Alternative and more cost-effective acceptors should be studied. For example, chlorate may be a potential candidate. It is a waste product from a variety of industries, a highly energetic electron acceptor, and commonly used by bacteria in activated sludge (Bryan. & Rohlich 1954). Finally, further research should confirm that nitrate addition will not lead to formation of undesirable denitrification intermediates, such as nitric or nitrous oxide (Rassamee *et al.* 2011). Nevertheless, from sustainability assessments, it has been observed that MBBRs shown relatively fewer environmental burdens compared to other existing biological treatment techniques (Gupta *et al.* 2022).

4. CONCLUSIONS

Our research suggests the MBBR is an effective option for treating winery wastewater. In particular, the addition of nitrate as both a nitrogen source and electron acceptor can substantially increase COD removal fluxes. Experimental and modelling results suggest that nitrate addition enhances COD degradation in the deeper, anoxic regions of the biofilm. Thus, nitrate addition may be cost-effective for 'peak shaving' during seasonal peak loadings.

ACKNOWLEDGEMENTS

We greatly appreciate the financial support provided by Corfo, Vinnova S.A. and the Chilean Government through ANID research grants FONDECYT 1200984 and PIA/BASAL FB0002.

DATA AVAILABILITY STATEMENT

All relevant data are included in the paper or its Supplementary Information.

CONFLICT OF INTEREST

The authors declare there is no conflict.

REFERENCES

Andreottola, G., Foladori, P., Ragazzi, M. & Villa, R. 2002 Treatment of winery wastewater in a sequencing batch biofilm reactor. *Water Sci. Technol.* **45** (12), 347–354. https://doi.org/10.2166/wst.2002.0445.

Andreottola, G., Foladori, P., Nardelli, P. & Denicolo, A. 2005 Treatment of winery wastewater in a full-scale fixed bed biofilm reactor. *Water Sci. Technol.* **51** (1), 71–79. https://doi.org/10.2166/wst.2005.0009.

Andreottola, G., Foladori, P. & Ziglio, G. 2009 Biological treatment of winery wastewater: An overview. *Water Sci. Technol.* **60** (5), 1117–1125. https://doi.org/10.2166/wst.2009.551.

APHA/AWWA/WEF 2005 *Standard Methods for the Examination of Water and Wastewater*, 21st edn. American Public Health Association/ American Water Works Association/Water Environment Federation, Washington, DC, USA.

Artiga, P., Carballa, M., Garrido, J. M. & Méndez, R. 2007 Treatment of winery wastewaters in a membrane submerged biorreactor. *Water Sci. Technol.* **56** (2), 63–69. https://doi.org/10.2166/wst.2007.473.

Aygun, A., Bilgehan, N. & Berktay, A. 2008 Influence of high organic loading rates on COD removal and sludge production in moving bed biofilm reactor. *Environ. Eng. Sci.* **25** (9), 1311–1316. https://doi.org/10.1089/ees.2007.0071.

Beck, C., Prades, G. & Sadowski, A. G. 2005 Activated sludge wastewater treatment plants optimization to face pollution overloads during grape harvest periods. *Water Sci. Technol.* **51** (1), 81–88. https://doi.org/10.2166/wst.2005.0010.

Bolzonella, D., Papa, M., Da Ros, C., Anga Muthukumar, L. & Rosso, D. 2019 Winery wastewater treatment: A critical overview of advanced biological processes. *Crit. Rev. Biotechnol.* **39** (4), 489–507. https://doi.org/10.1080/07388551.2019.1573799.

Bories, A., Guillot, J. M., Sire, Y., Couderc, M., Lemaire, S. A., Kreim, V. & Roux, J. C. 2007 Prevention of volatile fatty acids production and limitation of odours from winery wastewaters by denitrification. *Water Res.* **41** (13), 2987–2995. https://doi.org/10.1016/j.watres.2007.03.022.

Bryan, E. H. & Rohlich, G. A. 1954 Biological reduction of sodium chlorate as applied to measurement of sewage BOD. *Sewage Ind. Wastes.* **26** (11), 1315–1324. https://www.jstor.org/stable/25032612.

Chapman, J., Baker, P. & Wills, S. 2001 *Winery Wastewater Handbook: Production, Impacts and Management*. Winetitles, Adelaide, Australia.

Colin, T., Bories, A., Sire, Y. & Perrin, R. 2005 Treatment and valorisation of winery wastewater by a new biophysical process (ECCF). *Water Sci. Technol.* **51** (1), 99–106. https://doi.org/10.2166/wst.2005.0012.

Gupta, B., Gupta, A. K., Ghosal, P. S., Lal, S., Saidulu, D., Srivastava, A. & Upadhyay, M. 2022 Recent advances in application of moving bed biofilm reactor for wastewater treatment: Insights into critical operational parameters, modifications, field-scale performance, and sustainable aspects. *J. Environ. Chem. Eng.* **10** (3), 107742. https://doi.org/10.1016/j.jece.2022.107742.

Henze, M., Grady, C. P. L., Gujer, W., Marais, G. v. R. & Matsuo, T. 1987 *Activated Sludge Model No. 1. (IAWPRC Scientific and Technical Report No. 1)*. IWA Publishing, London, UK.

Jenkins, D., Richard, M. G. & Daigger, G. T. 2003 *Manual on the Causes of Activated Sludge Bulking, Foaming, and Other Solids Separation Problems*, 3rd edn. IWA Publishing, London, UK.

Jobbágy, A., Literáthy, B. & Tardy, G. 2002 Implementation of glycogen accumulating bacteria in treating nutrient-deficient wastewater. *Water Sci. Technol.* **46** (1–2), 185–190. https://doi.org/10.2166/wst.2002.0475.

Malandra, L., Wolfaardt, G., Zietsman, A. & Viljoen-Bloom, M. 2003 Microbiology of a biological contactor for winery wastewater treatment. *Water Res.* **37** (17), 4125–4134. https://doi.org/10.1016/S0043-1354(03)00339-7.

Ødegaard, H., Gisvold, B. & Strickland, J. 2000 The influence of carrier size and shape in the moving bed biofilm process. *Water Sci. Technol.* **41** (4–5), 383–391. https://doi.org/10.2166/wst.2000.0470.

Perry, R. H. & Green, D. W. 1997 *Perry's Chemical Engineers' Handbook*, 7th edn. McGraw-Hill, New York, NY, USA.

Petruccioli, M., Duarte, J. C. & Federici, F. 2000 High rate aerobic treatment of winery wastewater using bioreactors with free and immobilized activated sludge. *J. Biosci. Bioeng.* **90** (4), 381–386. https://doi.org/10.1016/S1389-1723(01)80005-0.

Rassamee, V., Sattayatewa, C., Pagilla, K. & Chandran, K. 2011 Effect of oxic and anoxic conditions on nitrous oxide emissions from nitrification and denitrification processes. *Biotechnol. Bioeng.* **108** (9), 2036–2045. https://doi.org/10.1002/bit.23147.

Reichert, P. 1998 *AQUASIM Version 2.0*. Swiss Federal Institute for Environmental Science and Technology (EAWAG), Dübendorf, Switzerland.

Reichert, P. & Wanner, O. 1997 Movement of solids in biofilms: Significance of liquid phase transport. *Water Sci. Technol.* **36** (1), 321–328. https://doi.org/10.1016/S0273-1223(97)00339-9.

Rodriguez, L., Villaseñor, J., Buendía, I. M. & Fernández, F. J. 2007 Reuse of winery wastewaters for biological nutrient removal. *Water Sci. Technol.* **56** (2), 95–102. https://doi.org/10.2166/wst.2007.477.

Spanjers, H., Vanrolleghem, P. A., Olsson, G. & Dold, P. L. 1998 *Respirometry in Control of the Activated Sludge Process: Principles*. IAWQ Scientific and Technical Report N° 7. IWA Publishing, London, UK.

Storm, D. R. 2001 *Winery Utilities: Planning, Design and Operation*. Aspen Publishers, New York, NY, USA.

Vanhooren, H., De Pauw, D. & Vanrolleghem, P. A. 2003 Induction of denitrification in a pilot-scale trickling filter by adding nitrate at high loading rate. *Water Sci. Technol.* **47** (11), 61–68. https://doi.org/10.2166/wst.2003.0587.

Wanner, O. & Gujer, W. 1986 A multispecies biofilm model. *Biotechnol. Bioeng.* **28** (3), 314–328. https://doi.org/10.1002/bit.260280304.

Wanner, O. & Morgenroth, E. 2004 Biofilm modeling with AQUASIM. *Water Sci. Technol.* **49** (11–12), 137–144. https://doi.org/10.2166/wst.2004.0824.

Wanner, O. & Reichert, P. 1996 Mathematical modeling of mixed-culture biofilms. *Biotechnol. Bioeng.* **49** (2), 172–184. https://doi.org/10.1002/(SICI)1097-0290(19960120)49:2 < 172::AID-BIT6 > 3.0.CO;2-N.

Yu, T. & Bishop, P. L. 2001 Stratification and oxidation-reduction potential change in an aerobic and sulfate-reducing biofilm studied using microelectrodes. *Water Environ. Res.* **73** (3), 368–373. https://doi.org/10.2175/106143001X139399.

First received 30 June 2023; accepted in revised form 1 February 2024. Available online 26 February 2024